Proc. Natl. Acad. Sci. USA
Vol. 86, pp. 9313–9317, December 1989
Cell Biology

Vectorial targeting of apical and basolateral plasma membrane proteins in a human adenocarcinoma epithelial cell line

ANDRÉ LE BIVIC*, FRANCISCO X. REAL†, AND ENRIQUE RODRIGUEZ-BOULAN*‡

*Department of Cell Biology and Anatomy, Cornell University Medical College, 1300 York Avenue, New York, NY 10021; and †Departamento de Immunologia, Institut Municipal d'Investigació Mèdica, Passeig Maritim 25-29, 08003-Barcelona, Spain

Communicated by George E. Palade, September 1, 1989

ABSTRACT **We studied the surface delivery pathways followed by newly synthesized plasma membrane proteins in intestinal cells. To this end, we developed an assay and characterized an epithelial cell line (SK-CO-15) derived from human colon adenocarcinoma. Polarized confluent monolayers (2000 Ω·cm^2), grown on polycarbonate filter chambers, were pulsed with radioactive methionine/cysteine and, at different times of chase, the protein fraction reaching the apical or basolateral surface was recovered by domain-selective biotinylation, immunoprecipitation, and immobilized streptavidin precipitation. Both an apical and a basolateral marker were found to be delivered vectorially to the respective surface, with a sorting efficiency of 50:1 for the basolateral marker and 14:1 for the apical marker.**

The mechanisms by which polarized epithelial cells sort and address plasma membrane proteins to apical and basolateral domains are still poorly understood (1–5). Research in different model epithelial systems has delineated two possible biogenetic pathways. In the kidney cell line MDCK (Madin–Darby canine kidney), exogenous viral envelope proteins are segregated intracellularly in the trans Golgi network and vectorially delivered by transport vesicles to their respective plasma membrane domains (6–9). An endogenous MDCK marker, the basolateral Na^+,K^+-ATPase, is also vectorially delivered (10). On the other hand, metabolic labeling/cell fractionation experiments with rat hepatocytes (11) and native intestinal cells (12–14) have provided evidence for initial delivery of both apical and basolateral antigens to the basolateral domain, followed by sorting and relocation of the apical proteins. However, Danielsen and Cowell (15) reported the opposite conclusion (i.e., intracellular sorting) for apical intestinal aminopeptidase, in agreement with electron microscopic studies that failed to detect these enzymes on the basolateral surface (16–18). Given the uncertainties arising from the different methodologies and epithelial cell systems used, it is unclear to what extent intracellular sorting or sorting at the plasma membrane are responsible for the sorting of apical and basolateral plasma membrane proteins in epithelial cells.

Here we have used a different approach (metabolic labeling combined with domain-selective biotinylation and recovery) to study the delivery of endogenous apical and basolateral antigens in a new polarized human colon adenocarcinoma cell line. This procedure avoids subcellular fractionation procedures, which is difficult in cultured cells, and allows for simple and sensitive monitoring of the delivery of plasma membrane proteins from intracellular biogenetic pools to the respective plasma membrane domain.

MATERIALS AND METHODS

Reagents. Cell culture reagents were purchased from GIBCO. Affinity-purified antibodies, rabbit anti-mouse IgG, and rhodamine-conjugated goat anti-mouse IgG were purchased from Cappel Laboratories. Protein A-Sepharose was from Pharmacia, sulfo-*N*-hydroxysuccinimido–biotin (s-NHS–biotin), sulfosuccinimidyl 2-(biotinamido)ethyl-1,3-dithiopropionate (s-NHS-SS–biotin), and streptavidin–agarose beads were from Pierce. All other reagents were obtained from Sigma.

Cells, Antibodies, and Cell Culture. The following materials were donated: SK-CO-15 cells (Lloyd Old, Sloane–Kettering Institute, New York); Caco-2 cells (A. Zweibaum, Villejuif, France); monoclonal antibodies against isomaltase, sucrase, aminopeptidase N, maltase-glucoamylase, and lactase (A. Quaroni, Ithaca, NY, and B. Nichols, Houston); and polyclonal villin antibodies (D. Louvard, Paris). Monoclonal antibodies against Ag 517 and Ag 525 are described elsewhere (19–21). Caco-2 cells and SK-CO-15 cells were grown in Dulbecco's modified Eagle's medium (DMEM) supplemented with 10% fetal bovine serum (FBS), penicillin (50 milliunits/ml), streptomycin (50 μg/ml), and nonessential amino acids (1%). Medium was changed daily. For experiments, cells were grown on Transwells (Costar) and were used after 10 days.

Biotinylation. Biotinylation of monolayers on Transwells with s-NHS–biotin [0.5 mg/ml in phosphate-buffered saline per ml (PBS)] (22) was carried out twice in a row for 15 min with 0.5 ml/1.5 ml in the apical/basal chamber. Free biotin was blocked with 50 mM NH_4Cl/PBS with 0.1 mM Ca/1 mM Mg (PBS-CM).

Biotinylation with s-NHS-SS–biotin was as for s-NHS–biotin. Reduction of surface s-NHS–biotin was with 50 mM glutathione for 30 min (23), in 90 mM NaCl/1 mM $MgCl_2$/0.1 mM $CaCl_2$/60 mM NaOH/10% FBS.

Pulse–Chase Experiments. Cells were incubated for 30 min in DMEM without methionine/cysteine, pulsed for 20 min in the same medium containing 0.8 mCi of Tran^{35}S-label (ICN) per ml (1 Ci = 37 GBq) and 0.4 mCi of [^{35}S]cysteine (NEN) per ml as described (24). Cells were washed once with DMEM, chased in DMEM containing 10× cysteine/methionine, and stored at 4°C in $NaCO_3H$-free DMEM/20 mM Hepes/0.2% bovine serum albumin (BSA) before biotinylation.

Immunoprecipitation and Streptavidin Precipitation. Filters were excised and cells were solubilized in 1 ml of buffer A [150 mM NaCl/20 mM Tris·HCl, pH 8.0/5 mM EDTA/1% Triton X-100 (TX-100)/0.2% BSA/protease inhibitors (25)] for 1 hr under agitation. The extract was precleared by addition of 100 μl of a *Staphylococcus aureus* slurry [fixed bacteria, 50% (vol/vol), prewashed three times] (Pansorbin, Calbiochem) for 15 min and centrifugation at 15,000 × *g* for 10 min. The supernatant was incubated for 12 hr with protein A-Sepharose (10 mg/ml) precoated with rabbit anti-mouse

The publication costs of this article were defrayed in part by page charge payment. This article must therefore be hereby marked "*advertisement*" in accordance with 18 U.S.C. §1734 solely to indicate this fact.

Abbreviations: s-NHS–biotin, sulfo-*N*-hydroxysuccinimido–biotin; s-NHS-SS–biotin, sulfosuccinimidyl 2-(biotinamido)ethyl-1,3-dithiopropionate; endo H, endoglycosidase H.

‡To whom reprint requests should be addressed.

IgG plus monoclonal antibodies (diluted 1:100 from ascites fluid). After incubation, the beads were washed once with buffer A, three times with buffer B (150 mM NaCl/20 mM Tris·HCl, pH 8.0/5 mM EDTA/0.5% TX-100/0.1% $NaDodSO_4$/0.2% BSA), three times with buffer C (500 mM NaCl/20 mM Tris·HCl, pH 8.0/0.5% TX-100/0.2% BSA), and once with 50 mM Tris·HCl (pH 8.0). To recover the immunoprecipitated biotinylated antigens, the beads were boiled with 10 μl of 10% $NaDodSO_4$ for 5 min, diluted with buffer A (500 μl per tube), and centrifuged (1 min; 15,000 × *g*). The supernatants were incubated overnight with streptavidin–agarose beads (50 μl; 50% slurry). The beads were washed as described above and boiled in gel sample buffer, and the supernatant was analyzed by $NaDodSO_4$/6–16% PAGE (26). The dried gels were processed for fluorography as described (27). Antigen recovery was measured by pulsing the cells for 30 min (see above), chasing for 4 hr, and comparing the immunoprecipitated cpm (100%) with the cpm recovered after surface biotinylation, immunoprecipitation, and immobilized streptavidin precipitation. Values observed were 9% for Ag 517 and 33% for Ag 525. In some cases, immunoprecipitated antigens from biotinylated cells were blotted with ^{125}I-labeled streptavidin on nitrocellulose (22, 28, 29). Triton X-114 extraction/phase separation (29) and endoglycosidase F/endoglycosidase H (endo H) digestions were performed as described (30, 31).

Frozen Sections and Transmission Electron Microscopy. Frozen sections (0.5 μm) of monolayers on collagen (20, 32) were processed for immunofluorescence as described (33). Cells grown on filters for 10 days were fixed with 2% glutaraldehyde/1% formaldehyde and were processed for transmission electron microscopy as reported (34).

RESULTS

SK-CO-15 monolayers displayed typical polarized epithelial properties: they developed numerous domes on plastic, like MDCK cells (35), typical junctional complexes, and sparse microvilli (Fig. 1*a*) different from the regular brush border (Fig. 1*b*) of Caco-2 cells (36). When grown on Transwells for 10 days, <1% of [^{3}H]inulin in 2 hr at 37°C diffused across the monolayer and a transepithelial resistance of 2300 + 922 (SD) Ω·cm^2, characteristic of an electrically "tight" epithelium, was measured. SK-CO-15 cells did not express sucrase-isomaltase, aminopeptidase N, lactase, glucoamylase, as observed by immunofluorescence; control Caco-2 monolayers expressed large amounts of these small intestine differentiation markers (not shown), as reported (35). Other differences with Caco-2 cells were 100 times less alkaline phosphatase activity and much lower villin levels (by immunoblot), consistent with the absence of brush border in SK-CO-15 cells (37).

Protein Composition of Apical and Basolateral Domains of SK-CO-15 Cells. Biotinylation of monolayers confluent for 10 days on Transwells demonstrated different patterns of integral and peripheral membrane proteins (not shown), as in MDCK cells (22). Immunofluorescence on semithin frozen sections with two monoclonal antibodies (19, 21) revealed a polarized distribution similar to that of the original glycoprotein antigens in human colon—i.e., apical for Ag 517 (stained 50% of the cells) and basolateral for Ag 525 (Fig. 2). When immunoprecipitated from cells pulsed for 3 hr with [^{35}S]methionine/[^{35}S]cysteine, Ag 525 appeared as 38- and 40-kDa bands that shifted to a single 36-kDa band after endoglycosidase F digestion (Fig. 3*B*). Ag 517 appeared as a main 190-kDa band and two minor 160- and 80-kDa bands; upon endoglycosidase F digestion these shifted to 110, 85, 60, and 36 kDa, consistent with Ag 517 being heavily glycosylated and multiform (19, 20).

By immunoprecipitation from monolayers biotinylated from each side with s-NHS–biotin, analyzed by $NaDodSO_4$ and blotted with ^{125}I-labeled streptavidin (Fig. 3*A*), the surface distributions of both antigens were confirmed. By counting the excised bands, 89% of Ag 517 was apical and 96% of Ag 525 was basolateral. Surface Ag 517 appeared as a main 190-kDa band and as minor 110- and 80-kDa bands. Ag 525 was present as a 38/40-kDa doublet and occasional degradation products (Fig. 3*A*, open arrowhead).

Biosynthesis and Surface Delivery of Ag 517 and Ag 525. SK-CO-15 cells on Transwells were pulsed for 20 min with [^{35}S]cysteine and [^{35}S]methionine and chased for various times. Ag 517 and Ag 525 were immunoprecipitated and subjected to endo H digestion (Fig. 4 *A* and *B*). Ag 525 had a single 38-kDa endo H-sensitive precursor that converted between a 20- to 40-min chase into a 38/40-kDa doublet, with both forms still sensitive to endo H, suggesting a heterogeneous glycosylation of mature Ag 525. Both forms were expressed at the cell surface (Fig. 4*D Right*). Ag 517 was present as three endo H-sensitive precursor bands with apparent molecular masses of 160, 100, and 55 kDa (Fig. 4*A*) that were processed to three mature forms of 190, 110, and 80 kDa between 40 and 80 min; 190 kDa was the major product expressed on the cell surface (Fig. 4*C*).

To follow the appearance at the cell surface of the two newly synthesized antigens, we used radioactive pulse–chase and surface-domain selective biotinylation of SK-CO-15 monolayers at different times of the chase. Ag 517 and Ag 525 were immunoprecipitated and the purified antigens were resuspended and reprecipitated with streptavidin coupled to agarose beads. The precipitated biotinylated antigens were then analyzed by $NaDodSO_4$/PAGE fluorography (Fig. 4 *C* and *D*). Ag 525 was initially detected at the basolateral surface after 30 min of chase and continued to appear with a half-time of 55 min (Fig. 5). Very little Ag 525 was detected on the apical membrane at any time of the chase (<2%) (Fig. 5). Interestingly, there was only ≈10 min delay between processing of Ag 525 to endo H resistance and its appearance at the basolateral surface, indicating that transport of this

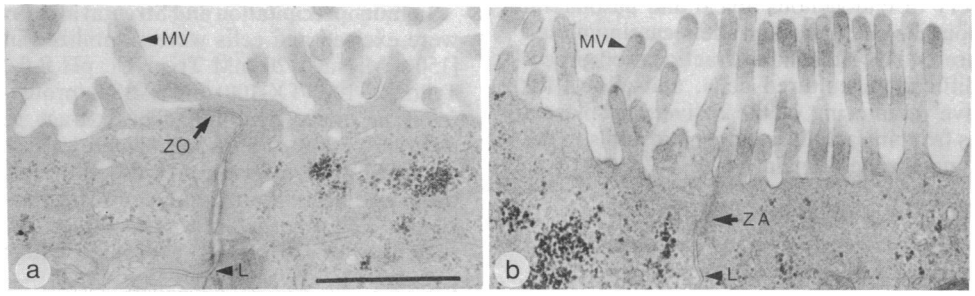

FIG. 1. Transmission electron microscopy of the apical surface of SK-CO-15 cells (*a*) and CaCo-2 cells (*b*). MV, microvilli; L, lateral membrane; ZO, zonula occludens; ZA, zonula adherens. Both cells exhibit junctional complexes but SK-CO-15 cells lack a typical brush border. (Bar = 1 μm.)

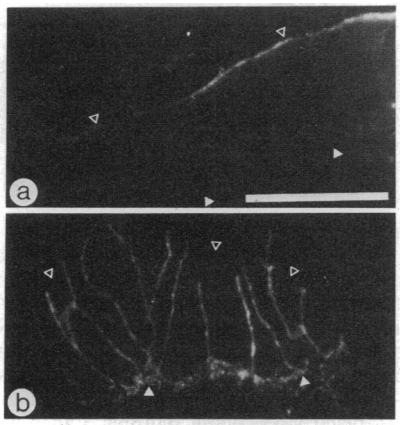

FIG. 2. Indirect immunofluorescence localization of Ag 517 (*a*) and Ag 525 (*b*) on semithin frozen sections of SK-CO-15 cells grown on collagen. Ag 517 is restricted to the apical side of the cells (open arrowheads), while Ag 525 is present only on the basolateral membrane (solid arrowheads). (Bar = 10 μm.)

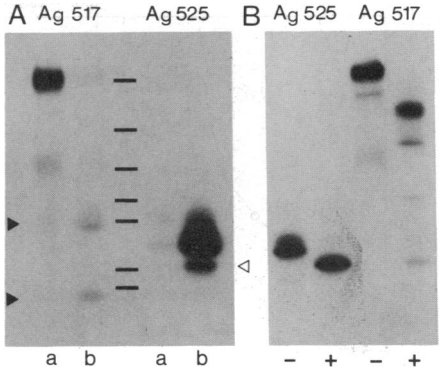

FIG. 3. (*A*) Immunoprecipitation of Ag 525 and Ag 517 after s-NHS–biotin labeling of apical (lanes a) or basolateral (lanes b) surface of SK-CO-15 monolayers. Ag 517 and Ag 525 were revealed, after $NaDodSO_4$/6–16% PAGE and transfer to nitrocellulose, by ^{125}I-labeled streptavidin. Solid arrowheads denote nonspecific binding of IgG heavy and light chain to ^{125}I-labeled streptavidin. Open arrowhead indicates a degradation product of Ag 525. Molecular masses from top to bottom are 180, 116, 82, 58, 48, 36, and 26 kDa. (*B*) Immunoprecipitation of Ag 525 and Ag 517 after 3 hr of labeling with [^{35}S]methionine and [^{35}S]cysteine (0.2 mCi/ml). Immunoprecipitates were treated with (lanes +) or without (lanes −) endoglycosidase F, run on $NaDodSO_4$/6–16% polyacrylamide gels, and processed for fluorography.

antigen between Golgi complex and the cell surface is very fast.

The initial surface appearance of Ag 517 was after 60 min of chase (Fig. 5). At that early time, there was already more Ag 517 present on the apical membrane than on the basolateral one (Fig. 5). Ag 517 accumulated on the apical membrane with a half-time of ≈120 min; no transient peak could be observed on the basolateral membrane, where the level of Ag 517 remained constant after 60 min of chase at a level of 5–7% of the total surface-expressed antigen (Fig. 5). Unlike Ag 525, there was a clear lag between acquisition of endo H resistance and surface appearance of Ag 517.

Fate of the Basolateral Pool of Ag 517. To study directly the fate of the basolateral pool of Ag 517, we used the reducible biotin analog s-NHS-SS–biotin. After biotinylation of the basolateral membrane at 4°C, cells were warmed to 37°C and the endocytosed or transcytosed fractions of Ag 517 were determined by reduction with glutathione from the same or the opposite (apical) side. The results indicate that Ag 517 was endocytosed slowly (Fig. 6, lanes j–l) and was poorly transcytosed (lanes m–o). Given that only 7% of Ag 517 is basolateral, this fraction cannot be a precursor to the apical antigen.

DISCUSSION

We have used different experimental approaches to study the biogenesis, surface delivery, and recycling of two polarized human colonic surface markers (20) in a new human adenocarcinoma intestinal cell line, SK-CO-15, which forms tight polarized epithelial monolayers in culture. We used a surface targeting assay that combines a pulse–chase protocol with domain-selective biotinylation (22) and recovery of the biotinylated (surface exposed) fraction of a specific antigen by successive immunoprecipitation and streptavidin–agarose precipitation. Compared with targeting assays previously

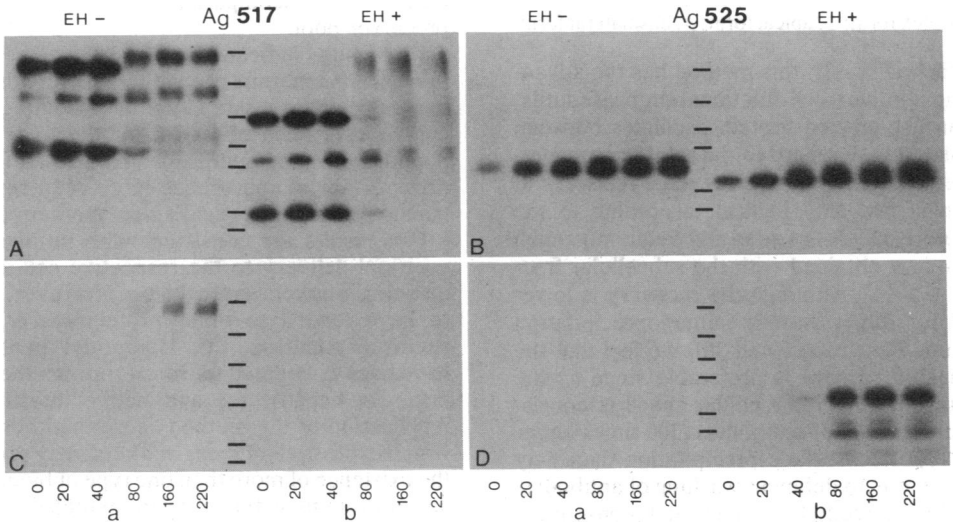

FIG. 4. Time course of endo H resistance (*A* and *B*) and appearance at the cell surface (*C* and *D*) of Ag 517 (*A* and *C*) and Ag 525 (*B* and *D*) in SK-CO-15 cells. Cells were pulsed with [^{35}S]methionine and [^{35}S]cysteine (0.8 and 0.4 mCi/ml, respectively) for 20 min and chased for various times. (*A*) Ag 517 immunoprecipitated and digested with (EH+) or without (EH−) endo H. (*B*) Ag 525 immunoprecipitated and digested with (EH+) or without (EH−) endo H. (*C*) Detection of newly synthesized Ag 517 at the apical surface (*a*) and on the basolateral surface (*b*) as described. (*D*) Detection of newly synthesized Ag 525 on the apical surface (*a*) and basolateral surface (*b*). $NaDodSO_4$/6–16% PAGE. Molecular masses are the same as in Fig. 3 except in *B* and *D*, where the 180-kDa marker is not shown.

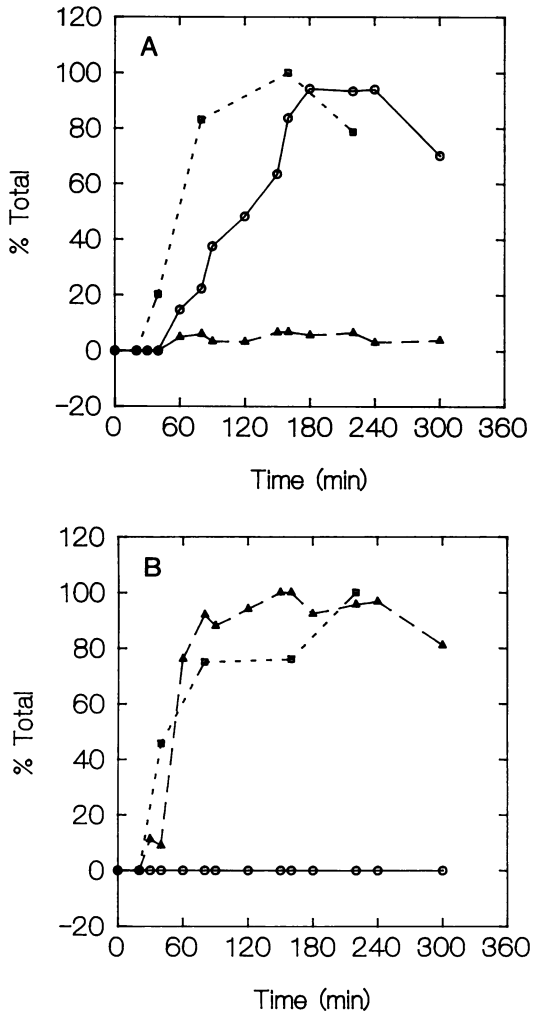

FIG. 5. Maturation and appearance at the cell surface of Ag 517 (*A*) and Ag 525 (*B*). Results from three pulse–chase experiments are shown. Fluorograms were scanned as described and the results are expressed as a percentage of the amount in the time point with the maximal expression. For Ag 517, the major product expressed at the cell surface, the 190-kDa band, and its endo H derivative (160 kDa) were scanned. □, Complex form; ○, apical form; △, basolateral form.

used on native epithelia (11–13), this method has the advantage of not requiring complex cell-fractionation procedures. Recovery of the surface-labeled protein oscillates between 9% and 33% (calculated with regard to the total immunoprecipitable cell antigen; therefore, the percentage recovery of the surface antigen is probably higher), according to the protein and is, therefore, at least as good and frequently much better than the recovery obtained with the subcellular fractionation protocols (11–14). Although the recovery is lower than that reported for direct surface immunoprecipitation with antibodies (up to 70%; refs. 9 and 38), we feel that the biotin procedure described here is preferable since (*i*) the penetration of biotin into the intercellular space is consistently more reliable than that of antibodies (300 times larger mass) and (*ii*) the reported surface precipitation data may overestimate recovery due to deficient washing of antibodies trapped in the filter/intercellular spaces and consequent precipitation of intracellular antigen during extraction.

Using the biotin targeting assay, both antigens appeared to be delivered vectorially to the respective surface. Delivery of Ag 525 to the basolateral surface occurred 10–15 min after maturation in the Golgi (as assessed by endo H resistance) and was strictly polarized (50:1). The delivery of apical Ag

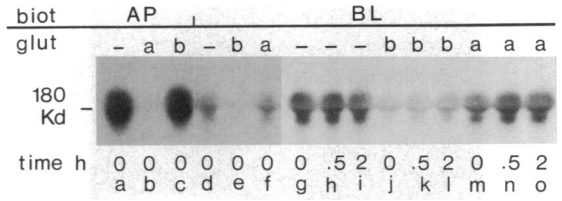

FIG. 6. Fate of basolateral Ag 517. Endocytosis and transcytosis of basolateral Ag 517 were studied by using a procedure derived from Bretscher and Lutter (23). Confluent SK-CO-15 monolayers were labeled with s-NHS-SS–biotin (biot) from the apical (AP) or basolateral (BL) side at 4°C and reduced with glutathione (glut) from the apical (a) or basolateral (b) side, immediately or after incubation at 37°C for 0.5 or 2 hr. Ag 517 was immunoprecipitated, separated by $NaDodSO_4$/6–12% PAGE under nonreducing conditions, and revealed by ^{125}I-labeled streptavidin blotting. Lanes a–f, note that polarity of Ag 517 is the same as that observed with s-NHS–biotin (Fig. 3); reduction is efficient only when performed from the same side as biotinylation. Lanes g–o, exposure time for these lanes is 3 times longer than for lanes a–f. After warming to 37°C, only a small fraction of Ag 517 was endocytosed (lanes j–l) and no transcytosis could be detected (lanes m–o). A background level of nonspecific ^{125}I-labeled streptavidin binding (lane j) is given by comigrating unreduced IgG (see also Fig. 3).

517 to the surface showed some important differences. First, a greater lag was observed between acquisition of endo H resistance ($t_{1/2}$ = 60 min) and appearance at the apical surface ($t_{1/2}$ = 120 min). Second, a larger percentage of this antigen (≈7%) was detected on the basolateral surface, indicating that sorting was less strict than for the basolateral Ag 525. The higher efficiency in the sorting of the basolateral marker Ag 525 agrees with previous estimates on the sorting efficiency of epithelial markers (2). The observed results are not compatible with a basolateral transient appearance of Ag 517 for two reasons: (*i*) at any time point of chase, there is more Ag 517 in the apical membrane than in the basolateral membrane and (*ii*) there is no visible basolateral Ag 517 peak before accumulation in the apical domain; rather, the basolateral level remains constant throughout the entire loading of the apical compartment, behaving as a stable missorted population. Furthermore, direct study of the basolateral pool of Ag 517 with a reducible biotin analog (Fig. 6) demonstrates long residence times and very small levels of endocytosis/transcytosis, incompatible with the behavior of an apical precursor pool.

Our results indicate that the delayed arrival of AG 517 to the apical membrane probably corresponds to a restriction in the transport at a late Golgi or post-Golgi step. Analogous delays have been observed for the transport of dipeptidyl peptidase IV and sucrase-isomaltase (37), and similar half-times of apical appearance have been reported for several hepatocyte and intestinal apical markers (11, 39, 40).

Our results are consistent with intracellular sorting and vectorial delivery to the respective cell surface of the two intestinal markers studied here. However, these results need to be extended to other proteins—e.g., aminopeptidase, sucrase-isomaltase, and dipeptidyl peptidase IV—which have been postulated to transit through the basolateral membrane in hepatocytes and native intestinal cells (11–14). Application of the methods described here to Caco-2 cells, which express all of these markers, may provide evidence for the existence of more than one type of biogenetic pathway for apical proteins within a given epithelial cell.

We thank Drs. A. Quaroni and B. Nichols for antibodies against human antigens used for control experiments; Drs. Eric Jaffe, Alejandro Schrott, Jeff Cheek, and Lutz Graeve for helpful discussions; Ms. Lori van Houten for photography; Ms. Lee Cohen-Gould for electron microscopy; and Ms. Francine Sanchez for help with typing the manuscript. This work was supported by National Insti-

tutes of Health Grant RO1-GM34107 and a New York Heart grant in aid. A.L.B. was supported by a fellowship from L'Association pour la Recherche sur le Cancer (France) and by UA179 CNRS (France). E.R.B. holds an Established Investigator Award from the American Heart Association.

1. Rodriguez-Boulan, E. (1983) *Mod. Cell Biol.* **1,** 119–170.
2. Simons, K. & Fuller, S. D. (1985) *Annu. Rev. Cell. Biol.* **1,** 243–288.
3. Matlin, K. S. (1986) *J. Cell Biol.* **103,** 2565–2568.
4. Bartles, J. R. & Hubbard, A. L. (1988) *Trends Biochem. Sci.* **13,** 181–184.
5. Rodriguez-Boulan, E. & Salas, P. J. I. (1989) *Annu. Rev. Physiol.* **51,** 741–754.
6. Misek, D. E., Bard, E. & Rodriguez-Boulan, E. (1984) *Cell* **39,** 537–546.
7. Matlin, K. S. & Simons, K. (1984) *J. Cell Biol.* **99,** 2131–2139.
8. Rindler, M. J., Ivanov, I. E., Plesken, H. & Sabatini, D. D. (1985) *J. Cell Biol.* **100,** 136–151.
9. Pfeiffer, S., Fuller, S. D. & Simons, K. (1986) *J. Cell Biol.* **101,** 470–476.
10. Caplan, M. J., Anderson, H. C., Palade, G. E. & Jamieson, J. D. (1986) *Cell* **46,** 623–631.
11. Bartles, J. R., Feracci, H. M., Stieger, B. & Hubbard, A. L. (1987) *J. Cell Biol.* **105,** 1241–1251.
12. Hauri, H. P., Quaroni, H. & Isselbacher, K. (1979) *Proc. Natl. Acad. Sci. USA* **76,** 5183–5186.
13. Massey, D., Feracci, H., Gorvel, J. P., Rigal, A., Soulie, J. M. & Maroux, S. (1987) *J. Membr. Biol.* **96,** 19–25.
14. Quaroni, A., Kirsch, K. & Weiser, M. M. (1979) *Biochem. J.* **182,** 203–212.
15. Danielsen, E. M. & Cowell, G. M. (1985) *Eur. J. Biochem.* **152,** 493–499.
16. Feracci, H., Bernadac, A., Gorvel, J. P. & Maroux, S. (1982) *Gastroenterology* **82,** 317–324.
17. Fransen, J., Guisel, L., Hauri, H. P., Sterchi, E. & Block, J. (1985) *Eur. J. Cell Biol.* **38,** 6–15.
18. Lorenzsonn, V., Korsmo, H. & Olsen, W. A. (1987) *Gastroenterology* **92,** 98–105.
19. Le Bivic, A., Hirn, M. & Reggio, H. (1987) *Biol. Cell.* **60,** 209–216.
20. Le Bivic, A., Hirn, M. & Reggio, H. (1988) *Proc. Natl. Acad. Sci. USA* **85,** 136–140.
21. Le Bivic, A., Bose-Biern, I. & Reggio, H. (1988) *Eur. J. Cell Biol.* **46,** 113–120.
22. Sargiacomo, M., Lisanti, M. P., Graeve, L., Le Bivic, A. & Rodriguez-Boulan, E. (1989) *J. Membr. Biol.* **107,** 277–286.
23. Bretscher, M. S. & Lutter, R. (1980) *EMBO J.* **7,** 4087–4092.
24. Mostov, K. E. & Deitcher, D. L. (1986) *Cell* **46,** 613–621.
25. Lisanti, M. P., Sargiacomo, M., Graeve, L., Saltiel, A. R. & Rodriguez-Boulan, E. (1988) *Proc. Natl. Acad. Sci. USA* **85,** 9557–9561.
26. Laemmli, U. K. (1970) *Nature (London)* **277,** 680–685.
27. Chamberlain, J. P. (1979) *Anal. Biochem.* **98,** 132–135.
28. Burnette, W. N. (1981) *Anal. Biochem.* **112,** 195–203.
29. Bordier, C. (1981) *J. Biol. Chem.* **256,** 1604–1607.
30. Tarentino, A. L. & Maley, F. (1974) *J. Biol. Chem.* **249,** 811–817.
31. Elder, J. H. & Alexander, S. (1982) *Proc. Natl. Acad. Sci. USA* **79,** 4540–4544.
32. Tokuyasu, K. T. (1973) *J. Cell Biol.* **57,** 551–565.
33. Reggio, H., Webster, P. & Louvard, D. (1983) *Methods Enzymol.* **98,** 379–395.
34. Rodriguez-Boulan, E. (1983) *Methods Enzymol.* **98,** 486–501.
35. Misfeldt, D. S., Hamamoto, S. T. & Pitelka, D. R. (1976) *Proc. Natl. Acad. Sci. USA* **73,** 1212–1216.
36. Pinto, M., Robine-Leon, S., Appay, M. D., Kedinger, M., Triadou, N., Dussaulx, E., Lacroix, B., Simon-Assmann, P., Haffen, K., Fogh, J. & Zweibaum, A. (1983) *Biol. Chem.* **47,** 323–330.
37. Dudouet, B., Robine, S., Huet, C., Sahuquillo-Merino, C., Blair, L., Coudrier, E. & Louvard, D. (1987) *J. Cell Biol.* **105,** 359–369.
38. Compton, T., Emanuilov Ivanov, I., Gottlieb, T., Rindler, M., Adesnik, M. & Sabatini, D. D. (1989) *Proc. Natl. Acad. Sci. USA* **86,** 4112–4116.
39. Stieger, B., Matter, K., Baur, B., Bucher, K., Hochli, M. & Hauri, H. P. (1988) *J. Cell Biol.* **106,** 1853–1861.
40. Eilers, U., Klumperman, J. & Hauri, H. P. (1989) *J. Cell Biol.* **108,** 13–22.